

The snake in the Brownian sphere

Omer Angel* Emmanuel Jacob† Brett Kolesnik‡
Grégory Miermont§

February 2025

Abstract

The Brownian sphere is a random metric space, homeomorphic to the two-dimensional sphere, which arises as the universal scaling limit of many types of random planar maps. The direct construction of the Brownian sphere is via a continuous analogue of the Cori–Vauquelin–Schaeffer (CVS) bijection. The CVS bijection maps labeled trees to planar maps, and the continuous version maps Aldous’ continuum random tree with Brownian labels (the Brownian snake) to the Brownian sphere. In this work, we describe the inverse of the continuous CVS bijection, by constructing the Brownian snake as a measurable function of the Brownian sphere. Special care is needed to work with the orientation of the Brownian sphere.

1 Introduction

The *Cori–Vauquelin–Schaeffer (CVS) bijection* [8, 24] is a correspondence between labeled trees and rooted and pointed quadrangulations of sphere, where by *pointed* we mean that an additional vertex, other than the root, has been distinguished. Given a (rooted and pointed) quadrangulation, the

*University of British Columbia, Department of Mathematics

†École Normale Supérieure de Lyon, Unité de Mathématiques Pures et Appliquées

‡University of Warwick, Department of Statistics

§École Normale Supérieure de Lyon, Unité de Mathématiques Pures et Appliquées, and Institut Universitaire de France

inverse CVS bijection yields a labeled plane tree, which is naturally embedded in the sphere, together with the map.

A continuum analogue of the CVS bijection may be obtained by associating a metric measure space (X, d, μ) with a pair of real-valued functions (f, g) , where f should be interpreted as the “contour function” of some \mathbb{R} -tree \mathcal{T}_f , and g as a label function defined on \mathcal{T}_f . When the pair of functions is random, with law given by the *Brownian snake* [11], the resulting random metric space is called the *Brownian sphere* [14, 19]. More specifically, taking f to be a normalized Brownian excursion, \mathcal{T}_f is *Aldous’ continuum random tree (CRT)* [1–3]. This random \mathbb{R} -tree is given Brownian labels g , which can be interpreted as Brownian motion indexed by the CRT. The Brownian sphere is a singular, spherical metric space (almost surely homeomorphic to the 2-dimensional sphere [16], but of Hausdorff dimension 4 [12]), which describes the scaling limit of many natural models of large planar maps of the sphere, as was first established by Le Gall [14] and Miermont [19].

The purpose of this work is to invert the continuum CVS mapping, so as to find the Brownian snake (and tree) in the Brownian sphere. While the Brownian sphere was first discovered as the scaling limit of random planar maps, it has since been constructed by other means, with connections to *Liouville quantum gravity* [21–23]. Therefore, our results further emphasize that the Brownian tree and snake are fundamental objects in modern probability, which present themselves, regardless of the way in which the Brownian sphere is constructed.

Our main result is the following.

Theorem 1. *Let (X, d, μ) be the Brownian sphere, and let x^0, x^1 be two independent points in X , drawn according to the measure μ . Then, almost surely, there exists a measurable function of (X, d, μ, x^0, x^1) , that outputs an \mathbb{R} -tree \mathcal{T} and a label function $Z : \mathcal{T} \rightarrow \mathbb{R}$, in such a way that:*

- (i) \mathcal{T} has the law of the CRT,
- (ii) Z are Brownian labels on \mathcal{T} , and
- (iii) the continuum CVS mapping applied to (\mathcal{T}, Z) recovers (X, d, μ) .

The last point of the theorem requires some interpretation, because the continuum CVS mapping will formally be defined on pairs of functions encoding (\mathcal{T}, Z) , which endow the tree \mathcal{T} with some extra structure; namely, with a certain “planar order.” See Theorem 4 below for a formal version of Theorem 1.

1.1 The construction

As we will see, the construction in Theorem 1 is quite natural. In order to describe the inverse continuum CVS mapping, we use the geometric notion of a *cut locus*. We recall that, if X is a geodesic metric space, the cut locus of X with respect to a point $x \in X$ is the set of all points z such that there are at least two distinct geodesics between z and x . Let $\mathcal{C}(X, d, x)$ denote the cut locus of the Brownian sphere (X, d) with respect to x . For the Brownian sphere, Le Gall [13] showed that, for μ -almost every x , the cut locus \mathcal{C} has measure 0, and is dense in X . The inverse continuum CVS mapping is constructed in several steps, as outlined below:

1. Given the doubly marked Brownian sphere (X, d, μ, x^0, x^1) , let $\mathcal{C} = \mathcal{C}(X, d, x^1)$ be the cut locus with respect to x^1 .
2. For each point $y \in \mathcal{C}$, define $Z(y) = d(y, x^1) - d(x^0, x^1)$.
3. Observe that (\mathcal{C}, d) is almost surely (a.s.) path-connected and has no cycles. By local connectivity there is a topology on \mathcal{C} in which it is a dendrite embedded in the Brownian sphere.
4. Observe that \mathcal{C} does not include the leaves of the dendrite, however, the labels Z extend continuously to the closure \mathcal{T} of \mathcal{C} with respect to a local topology, intrinsic to \mathcal{C} .
5. Define a metric on \mathcal{T} so that $Z : \mathcal{T} \rightarrow \mathbb{R}$ is a Brownian motion indexed by \mathcal{T} . To find the distance, note that $d_{\mathcal{T}}(u, v)$ is the quadratic variation of the function Z along the unique path between u and v in \mathcal{T} .
6. The orientation of the Brownian sphere induces an order on \mathcal{T} , making it a plane tree, and thereby canonically encoded by a contour process.

These steps will be justified in Section 4, where we will also address the delicate question of the measurability of the resulting mapping. Let us discuss a little more the role of the marked points and of the orientation in the construction.

1.2 The marked points

The two marked points x^0, x^1 indeed play a crucial role in the recovery of the label process. Roughly speaking, we will use one marked point to determine its “time origin,” and the other marked point for its values.

The roles of x^0 and x^1 are very different in the mapping that we construct. For a given space (X, d, μ, x^0, x^1) as in Theorem 1, a change of x^0 amounts to a re-rooting of the tree \mathcal{T} . A change in x^1 , on the other hand, modifies the

tree and process Z profoundly. Roughly, the tree is cut into countably many trees, which are then reconnected in a different manner, while maintaining the increments of Z on each part.

We note that the Brownian sphere usually comes equipped with a distinguished point ρ , called the *root*. By Le Gall’s [13] *re-rooting property*, ρ is equal in distribution to a random point x drawn according to the measure μ . The two marked points x^0, x^1 in our construction are independent, with the same distribution as ρ .

1.3 Choosing an orientation

The choice of an orientation for the Brownian sphere also plays a crucial role in our construction. The Brownian sphere is homeomorphic to a sphere, and thus orientable. Previous works, however, have mostly avoided explicitly discussing the issue of orientation.

Both constructions of the Brownian sphere, as a quotient of the CRT or via Liouville quantum gravity, give rise to a natural orientation of the sphere. However, if we are given the Brownian sphere as an unoriented metric space, there are two possible orientations. Reversing the orientation of the sphere corresponds to a reflection of the CRT.

It is worth explaining what we mean when discussing the Brownian sphere as an oriented space. It is not a smooth manifold, so some standard definitions fail. There are several possible equivalent definitions for the orientation of a topological sphere X :

1. For each simple loop we may regard one side as the interior and the other as the exterior, making the choice continuously on the space of loops in X .
2. For each collection of pairwise disjoint paths emanating from $x \in X$, we can determine a cyclic order, again making the choice continuously on the space of such “stars.”
3. Observe that the homology group $H_2(X, \mathbb{Z})$ is isomorphic to \mathbb{Z} , and select one of the generators as $+1$ and the other as -1 .

Of these, the first and third extend naturally to higher dimensions. The first two are “local” and generalize to topologies other than the sphere. In the case of a topological sphere, these definitions are all equivalent.

To deal with the fact that the Brownian sphere has been defined as an *unoriented* metric space, there are two approaches that one might take. One could consider the Brownian sphere as an oriented metric space to begin

with. This would require revisiting the definition of the Brownian sphere, and to view it as a random element of a space of oriented metric spheres. Working in such an abstract space would create some undesirable technicalities. Specifically, a number of steps in the construction of the Brownian sphere would need to be revisited to show that all steps work with oriented spheres. For example, Le Gall and Paulin [16] used Moore’s theorem to show that the Brownian sphere is homeomorphic to the sphere. The usual form of Moore’s theorem does not provide an orientation for the quotient space, though one can verify that there is a natural orientation.

Another approach, which we will follow, is to simply consider the Brownian sphere as a metric space, and assign to it a random orientation based on an independent variable $\epsilon \in \{\pm 1\}$, to account for the two possible orientations. This is conceptually simpler, but poses some measurability issues that will need to be addressed.

1.4 Other Brownian surfaces

The Brownian sphere is only one element in a family of compact [5, 6] or non-compact [4, 9] Brownian random surfaces, including the Brownian plane, disc, and any compact orientable surface with or without boundary. Although we did not work out the details, we are confident that the methods and results of this paper generalize to these objects with little change, and similar inverse bijections to that of Theorems 1 and 4 can be derived in these settings, because Brownian random surfaces all have similar constructions in terms of labeled tree-like structures.

For instance, the *Brownian plane* [9], which is a random pointed metric measure space (X, d, μ, x^0) that is a.s. homeomorphic to \mathbb{R}^2 , is obtained if the Brownian excursion used to generate the CRT is replaced by a two-sided, infinite Brownian motion encoding the infinite, self-similar CRT, see e.g. [4]. In this setting, the second marked point x^1 can be taken to be at infinity. The labels Z are well-defined, since there is a unique Busemann function $B_{x^0}(x) = d(x, \infty) - d(x^0, \infty)$ on the Brownian plane, and the cut locus with respect to infinity is the set of points from which one can start multiple geodesics rays. From these basic facts, one should be able apply the methods of Section 4 with little change. In this situation, however, the “orientation” random variable ϵ_n appearing below in (3) would need to be defined in some other way, but fortunately, there is some flexibility in its choice, see the last remark of Section 3.1.

1.5 Organization of the paper

The rest of the paper consists of three sections. In Section 2, we review the basic constructions of the Brownian tree, snake and sphere, and properly define the continuum Cori-Vauquelin-Schaeffer mapping that we want to invert. Section 3 states and discusses Theorem 4, a more precise version of Theorem 1, and shows how the latter follows from the former. Section 4 provides the proof of Theorem 4, following the steps in Section 1.1.

1.6 Acknowledgments

We thank Jean-François Le Gall for useful discussions. The authors would like to thank the Isaac Newton Institute for Mathematical Sciences, Cambridge, for support and hospitality during the program Random geometry, where initial work on this paper was undertaken. This work was supported by EPSRC grant EP/K032208/1. OA is supported in part by NSERC.

2 Random snakes and the Brownian sphere

We first review the definitions of some of the known objects we will work with, namely, the Brownian tree, snake and sphere, and the properties that will be needed in the proof of Theorem 4 below.

2.1 Deterministic encodings

Let us first give a general discussion on some metric structures encoded by deterministic functions.

2.1.1 Trees coded by functions

If $f : [0, 1] \rightarrow \mathbb{R}$ is a continuous function such that $f(0) = f(1) = 0$, we define

$$d_f(s, s') = f(s) + f(s') - 2 \max \left(\inf_{[s \wedge s', s \vee s']} f, \inf_{[0, s \wedge s'] \cup [s \vee s', 1]} f \right),$$

which defines a pseudometric on $[0, 1]$. This means that it is a symmetric function that satisfies the triangle inequality, and vanishes on the diagonal. In fact, we can alternatively view f as a function $f : \mathbb{S}^1 \rightarrow \mathbb{R}$, where the unit

circle \mathbb{S}^1 is identified with \mathbb{R}/\mathbb{Z} , and, with this identification, the expression for d_f simplifies to

$$d_f(s, s') = f(s) + f(s') - 2 \max \left(\inf_{[s, s']_\circ} f, \inf_{[s', s]_\circ} f \right),$$

where $[s, s']_\circ$ and $[s', s]_\circ$ are the two naturally oriented arcs of \mathbb{S}^1 between s and s' .

The quotient $\mathcal{T}_f = [0, 1]/\{d_f = 0\}$, endowed with the distance inherited from d_f , is an \mathbb{R} -tree, and for $a, b \in \mathcal{T}_f$, we denote by $[[a, b]]_f$ the unique geodesic segment between a and b in (\mathcal{T}_f, d_f) .

It naturally carries a distinguished point $\rho_f = p_f(\operatorname{argmin} f)$, where $p_f : [0, 1] \rightarrow \mathcal{T}_f$ is the quotient mapping. Note $d_f(s, t) = 0$ whenever f attains its infimum at s and t , so ρ_f is well defined.

We call $(\mathcal{T}_f, d_f, \rho_f)$ the *rooted tree coded by f* .

2.1.2 The mating of trees metric

Let us denote by \mathcal{S} the space of pairs $h = (f, g)$ of continuous functions $f, g : [0, 1] \rightarrow \mathbb{R}$, taking value 0 at 0 and 1. We associate with f and g the trees (\mathcal{T}_f, d_f) and (\mathcal{T}_g, d_g) as above¹.

For $h \in \mathcal{S}$, the *mating of trees pseudometric* is defined, for every s, t in $[0, 1]$, by

$$d_h(s, t) = \inf \left\{ \sum_{i=1}^k d_g(s_i, t_i) : \begin{array}{l} k \geq 1, s = s_1, t_1, s_2, t_2, \dots, s_k, t_k = t \\ d_f(t_j, s_{j+1}) = 0, 1 \leq j \leq k-1 \end{array} \right\}.$$

The quotient $X_h = [0, 1]/\{d_h = 0\}$, endowed with the distance inherited from d_h , is called the *mating of trees coded by h* . Informally, it is obtained by “wrapping” the tree (\mathcal{T}_g, d_g) around the tree \mathcal{T}_f . Note that the construction is not at all symmetric in the two trees. In particular, it depends strongly on d_g , but depends on f only through the set $\{d_f = 0\}$, that is, on the topological space \mathcal{T}_f .

¹In our applications below, starting with Section 2.3, we will require the further property that (f, g) encodes a “snake trajectory.” This means that g can be interpreted as a label function on the tree \mathcal{T}_f , in the sense that $g(s) = g(t)$ for any s, t such that $d_f(s, t) = 0$. However, we stress that the discussion of Section 2.1 holds in full generality.

As a consequence of the definition of the quotient metric d_h , there is a natural commutative diagram:

$$\begin{array}{ccc}
 [0, 1] & \xrightarrow{p_f} & \mathcal{T}_f \\
 \downarrow p_g & \searrow p_h & \downarrow \mathbf{p}_f \\
 \mathcal{T}_g & \xrightarrow{\mathbf{p}_g} & X_h
 \end{array} \tag{1}$$

All projection mappings $p_f, \mathbf{p}_f, p_g, \mathbf{p}_g, p_h$ are continuous. Therefore, X_h can be seen as the quotient of either \mathcal{T}_f or \mathcal{T}_g , with canonical projections $\mathbf{p}_f, \mathbf{p}_g$.

The space X_h naturally carries two distinguished points

$$x_h^0 = p_h(\operatorname{argmin} f) = \mathbf{p}_f(\rho_f) \quad \text{and} \quad x_h^1 = p_h(\operatorname{argmin} g) = \mathbf{p}_g(\rho_g),$$

where, we recall that ρ_f, ρ_g are the roots of the trees $\mathcal{T}_f, \mathcal{T}_g$.

We also define the image measure $\mu_h = (p_h)_* \operatorname{Leb}_{[0,1]}$, which we call the *area measure on X_h* .

2.1.3 Gromov–Hausdorff-type spaces

In order to consider random versions of the metric space constructions discussed above, with $h \in \mathcal{S}$ random, we will need to introduce Gromov–Hausdorff-type spaces.

Suppose that $(X, d_X, \mu_X, (a_i)_{1 \leq i \leq n})$ and $(Y, d_Y, \mu_Y, (b_i)_{1 \leq i \leq n})$ are two compact metric measure spaces with $n \geq 0$ distinguished points. We call them *isometric* if there exists an isometry $\varphi : (X, d_X) \rightarrow (Y, d_Y)$ such that $\mu_Y = \varphi_* \mu_X$ and $\varphi(a_i) = b_i$ for $1 \leq i \leq n$. We let $[X, d_X, \mu_X, (a_i)_{1 \leq i \leq n}]$ denote the isometry class of $(X, d_X, \mu_X, (a_i)_{1 \leq i \leq n})$. We endow the set $m\mathcal{M}^{n\bullet}$ of all such isometry classes with the Gromov–Hausdorff–Prokhorov topology. We write $\mathbf{X}^{n\bullet}$ to denote a generic element of $m\mathcal{M}^{n\bullet}$, to emphasize that it has n marked points. When $n = 0$, we write $m\mathcal{M} = m\mathcal{M}^{0\bullet}$ and $\mathbf{X} = \mathbf{X}^{0\bullet}$. In Section 3.3 below, we will also consider the Gromov–Hausdorff space \mathcal{M} of isometry classes $[X, d]$ of compact metric spaces, endowed with the Gromov–Hausdorff topology.

In particular, for every $h \in \mathcal{S}$, the isometry class $[X_h, d_h, \mu_h, x_h^0, x_h^1]$ is an element of $m\mathcal{M}^{2\bullet}$, which we denote by $\mathbf{X}_h^{2\bullet}$. We also let $\mathbf{X}_h = [X_h, d_h, \mu_h]$ be its unmarked version.

2.2 The continuum CVS mapping ψ

Finally, using the above definitions, we obtain a mapping

$$\psi : \begin{array}{l} \mathcal{S} \longrightarrow m\mathcal{M}^{2\bullet} \\ h \longmapsto \mathbf{X}_h^{2\bullet}, \end{array} \quad (2)$$

which we call the *continuum CVS mapping*.

Proposition 2. *The continuum CVS mapping is measurable.*

Proof. Let \mathcal{C}_m be the space of continuous functions from $[0, 1]^2$ to \mathbb{R}_+ that are pseudometrics. Consider the mapping

$$\psi_1 : \begin{array}{l} \mathcal{S} \longrightarrow \mathcal{C}_m \times [0, 1] \times [0, 1] \\ h = (f, g) \longmapsto ((d_h(s, t), 0 \leq s, t \leq 1), s_*(f), s_*(g)), \end{array}$$

where $s_*(f)$ (resp. $s_*(g)$) is the first times that f (resp. g) attains its minimum. We already mentioned that d_h is a pseudometric. The fact that it is continuous can be seen by writing

$$|d_h(s, t) - d_h(s', t')| \leq d_h(s, s') + d_h(t, t') \leq d_g(s, s') + d_g(t, t'),$$

which goes to 0 as $(s', t') \rightarrow (s, t)$. Moreover, for a fixed integer $k \geq 1$, for $\delta > 0$ and for $s, t \in [0, 1]$, the quantities

$$d_h^{(k, \delta)}(s, t) = \inf \left\{ \sum_{i=1}^k d_g(s_i, t_i) : \begin{array}{l} s = s_1, t_1, s_2, t_2, \dots, s_k, t_k = t \\ d_f(t_j, s_{j+1}) < \delta, 1 \leq j \leq k-1 \end{array} \right\}$$

are measurable functions of h (note that the infimum can be taken over choices of $t_1, s_2, t_2, \dots, s_k$ in \mathbb{Q}), so that the same holds for $d_h(s, t)$, since it equals $\lim_{k \rightarrow \infty} \lim_{\delta \downarrow 0} d_h^{(k, \delta)}(s, t)$. The measurability of ψ_1 follows.

Finally, consider the mapping

$$\psi_2 : \begin{array}{l} \mathcal{C}_m \times [0, 1] \times [0, 1] \longrightarrow m\mathcal{M}^{2\bullet} \\ (d, s, t) \longmapsto [[0, 1]/\{d = 0\}, d, p_*\text{Leb}, p(s), p(t)] \end{array},$$

where for $d \in \mathcal{C}_m$, the mapping $p : [0, 1] \rightarrow [0, 1]/\{d = 0\}$ is the canonical projection map. This mapping is easily seen to be continuous. Altogether, we obtain the result, noting that $\psi = \psi_2 \circ \psi_1$. \blacksquare

The following lemma is a simple but important observation. For $h \in \mathcal{S}$, we denote by $R(h)$ the reversed path $(f(1 - \cdot), g(1 - \cdot))$.

Lemma 3. *For every $h \in \mathcal{S}$, the spaces $\mathbf{X}_h^{2\bullet}$ and $\mathbf{X}_{R(h)}^{2\bullet}$ are equal as elements of $m\mathcal{M}^{2\bullet}$.*

The proof is immediate, noting that $s \in [0, 1] \mapsto 1 - s$ induces an isometry between $(X_h, d_h, \mu_h, x_h^0, x_h^1)$ and $(X_{R(h)}, d_{R(h)}, \mu_{R(h)}, x_{R(h)}^0, x_{R(h)}^1)$. We remark that if one considers the quotient spaces as oriented spheres, then $\mathbf{X}_{R(h)}^{2\bullet}$ is the reflection of $\mathbf{X}_h^{2\bullet}$, i.e. the same space with the opposite orientation.

2.3 The Brownian tree, snake and sphere

The Brownian tree, snake and sphere are obtained by applying the above constructions to certain natural random functions.

Let $(\mathbf{e}_t, 0 \leq t \leq 1)$ be a normalized Brownian excursion. The tree $(\mathcal{T}_{\mathbf{e}}, d_{\mathbf{e}})$ that it encodes is called Aldous' *continuum random tree* (CRT). The Brownian excursion is nonnegative, so its root is simply $\rho_{\mathbf{e}} = p_{\mathbf{e}}(0)$.

Next, conditionally given \mathbf{e} , define a continuous centered Gaussian process $(Z_t, 0 \leq t \leq 1)$ with covariance function

$$\text{Cov}(Z_s, Z_t) = \inf_{s \wedge t \leq u \leq s \vee t} \mathbf{e}_u.$$

The fact that such a process has a continuous version is well known. Moreover, almost surely, $Z_s = Z_t$ for every s, t such that $d_{\mathbf{e}}(s, t) = 0$, so that Z can be seen as a process indexed by $\mathcal{T}_{\mathbf{e}}$. Indeed, this process can be interpreted as Brownian motion indexed by $\mathcal{T}_{\mathbf{e}}$, with value 0 at $\rho_{\mathbf{e}}$, and with independent increments over disjoint paths. The pair $W = (\mathbf{e}, Z)$ is a random element of \mathcal{S} , which we call the *Brownian snake*². Its law is denoted by $\mathbb{P}_{\text{Snake}}$.

Finally, applying the continuum CVS mapping $\psi : h \mapsto \mathbf{X}_h^{2\bullet}$ to the Brownian snake, we obtain the (doubly marked) *Brownian sphere* $\mathbf{X}_W^{2\bullet}$, with values in $m\mathcal{M}^{2\bullet}$. We denote its law by $\mathbb{P}_{\text{Sphere}}^{2\bullet} = \psi_* \mathbb{P}_{\text{Snake}}$. We also denote by $\mathbb{P}_{\text{Sphere}}$ the law of the *unmarked* Brownian sphere \mathbf{X}_W , with values in $m\mathcal{M}$.

²In fact, what is usually called the *Brownian snake* is the path-valued Markov process encoding the trajectories of Z from the root of $\mathcal{T}_{\mathbf{e}}$, as one follows the contour of the tree. The process \mathbf{e} is called the *lifetime process* of the snake, and Z the *head of the snake*. However, this path-valued process can be recovered as a continuous function of (\mathbf{e}, Z) .

3 The inverse continuum CVS mapping ϕ

Our goal is to invert the continuum CVS mapping, that is, to find a measurable mapping $m\mathcal{M}^{2\bullet} \rightarrow \mathcal{S}$ that is an (almost sure) inverse of ψ

One possible approach is as follows. Suppose we find a Borel subset $A \subset \mathcal{S}$ such that $\mathbb{P}_{\text{Snake}}(\mathcal{S} \setminus A) = 0$ and $\psi|_A$ is injective. Then, by a general theorem of Lusin and Souslin on measurable functions on Polish spaces (see, e.g., Kechris [10, Corollary 15.2]), it would follow that $\psi(A) \subset m\mathcal{M}^{2\bullet}$ is a Borel set, and that the inverse $\phi : \psi(A) \rightarrow A$ is Borel measurable.

This approach, however, has two major drawbacks. First, it gives an abstract inverse function, without telling us anything about its nature or how to compute it. Secondly, this approach requires the continuum CVS mapping to be almost everywhere injective, which it is *not*, due to Lemma 3. Applying the reflection R , while preserving the planar tree structure and Brownian labels, has the effect of reversing the orientation of the Brownian sphere (as will be further discussed in Section 4.3). However, $m\mathcal{M}^{2\bullet}$ does not include information about the orientation of the sphere. Thus, as we will state and prove rigorously below (see Theorem 4), the continuum CVS mapping is actually 2-to-1 on a set of full probability for the law $\mathbb{P}_{\text{Snake}}$.

This is also the case for discrete maps, if one does not keep track of their orientation. This has not been an issue in the past since discrete maps have always been considered as oriented (not just orientable), so that a map and its reflection are considered as distinct objects. However, previous works on the Brownian sphere have opted to omit the orientation when taking the limit, so that a map and its reflection are considered identical.

To overcome this issue, we work in an extended space $m\mathcal{M}^{2\bullet} \times \{\pm 1\}$. The coordinate in $\{\pm 1\}$ is used to determine the *orientation* of the Brownian sphere. As one might expect, this orientation turns out to be uniformly random (see Proposition 5). However, as we will see, describing this choice in a *measurable* way requires some care.

For $h = (f, g) \in \mathcal{S}$, recall that $s_*(g)$ is the first time that g attains its minimum. We put

$$\epsilon_h = \text{sgn}(1 - 2s_*(g)) = \begin{cases} 1 & \text{if } s_*(g) \leq 1/2 \\ -1 & \text{if } s_*(g) > 1/2. \end{cases} \quad (3)$$

We then extend the mapping ψ by

$$\begin{aligned} \bar{\psi}: \mathcal{S} &\longrightarrow m\mathcal{M}^{2\bullet} \times \{\pm 1\} \\ h &\longmapsto (\psi(h), \epsilon_h). \end{aligned} \tag{4}$$

When $W = (\mathbf{e}, Z)$ follows the law of the Brownian snake, the infimum of Z is a.s. attained at the unique time $s_* = s_*(Z)$, as shown in [17, §2.3]. Since Z has cyclically exchangeable increments, this implies that s_* is uniformly distributed in $[0, 1]$, see [7, Corollary 3.1]. In particular, ϵ_W follows the Rademacher distribution (equal to ± 1 with equal probability).

We may finally state our main result in a precise form.

Theorem 4. *There exists a Borel mapping $\phi : m\mathcal{M}^{2\bullet} \times \{\pm 1\} \rightarrow \mathcal{S}$ which is an a.s. inverse of $\bar{\psi}$, in the sense that:*

(i) $\mathbb{P}_{\text{Sphere}}^{2\bullet}(d\mathbf{X}^{2\bullet})$ -a.s., and for every $\epsilon \in \{\pm 1\}$,

$$\bar{\psi} \circ \phi(\mathbf{X}^{2\bullet}, \epsilon) = (\mathbf{X}^{2\bullet}, \epsilon), \quad \text{and}$$

(ii) $\mathbb{P}_{\text{Snake}}(dh)$ -a.s.,

$$\phi \circ \bar{\psi}(h) = h.$$

This result immediately yields that, $\mathbb{P}_{\text{Sphere}}^{2\bullet}(d\mathbf{X}^{2\bullet})$ -a.s., for $\epsilon \in \{\pm 1\}$,

$$\psi \circ \phi(\mathbf{X}^{2\bullet}, \epsilon) = \mathbf{X}^{2\bullet},$$

which justifies our interpretation of ϕ as an inverse of the continuum CVS mapping ψ . See also (6) below for composing ϕ and ψ in the reverse order.

In the following subsections, we will explain why the above statement implies Theorem 1, which will also allow us to clarify the role of the parameter ϵ and of the two marked points that appear in the input of the mapping ϕ .

3.1 The role of ϵ

Let us first discuss the meaning of the parameter $\epsilon \in \{\pm 1\}$. We claim that, $\mathbb{P}_{\text{Snake}}(dh)$ -a.s.,

$$\bar{\psi}(R(h)) = (\psi(h), -\epsilon_h), \tag{5}$$

recalling that $R(h)$ is time-reversal of h . Indeed, as already mentioned, $\psi(h)$ and $\psi(R(h))$ are equal as elements of $m\mathcal{M}^{2\bullet}$. Also, $\epsilon_{R(h)} = -\epsilon_h$, $\mathbb{P}_{\text{Snake}}(dh)$ -a.s., because the law of $s_*(g)$ under $\mathbb{P}_{\text{Snake}}$ is diffuse, so that the probability

$s_*(g) = 1/2$ (and hence that $\epsilon_{R(h)} = \epsilon_h$) is zero. In particular, we deduce the following two properties. First, $\mathbb{P}_{\text{Snake}}(dh)$ -a.s., for $\epsilon \in \{\pm 1\}$,

$$\phi(\psi(h), \epsilon) \in \{h, R(h)\}. \quad (6)$$

Second, $\mathbb{P}_{\text{Sphere}}^{2\bullet}(d\mathbf{X}^{2\bullet})$ -a.s.,

$$\phi(\mathbf{X}^{2\bullet}, -\epsilon) = R(\phi(\mathbf{X}^{2\bullet}, \epsilon)), \quad \epsilon \in \{\pm 1\}. \quad (7)$$

These properties show that ϵ determines the ‘‘orientation’’ of h . As we will see in the course of the proof of Theorem 4, ϵ allows one to distinguish $\mathbb{P}_{\text{Snake}}$ -almost surely h from $R(h)$. Moreover, ϵ determines an orientation of $\psi(h)$, which under \mathbb{P}_h is a.s. a topological sphere, and this orientation is reversed by changing ϵ to $-\epsilon$. See Section 4.3 for more details.

Next, we describe the joint law of $(\psi(h), \epsilon_h)$ under $\mathbb{P}_{\text{Snake}}$.

Proposition 5. *Under $\mathbb{P}_{\text{Snake}}(dh)$, the random variables $\psi(h)$ and ϵ_h are independent, and the latter has the Rademacher distribution.*

Proof. We use the well-known (and easy to check) fact that $R(h)$ has same distribution as h under $\mathbb{P}_{\text{Snake}}$. Therefore, (5) implies that $(\psi(h), \epsilon_h)$ and $(\psi(h), -\epsilon_h)$ have same distribution under $\mathbb{P}_{\text{Snake}}$. Hence, the random variables $\pm\epsilon_h$ have the same law conditionally given $\psi(h)$. The result follows. \blacksquare

The above proposition and the discussion just before its statement are in line with the intuitive fact that, conditionally given the (orientable, but not oriented) random sphere $\mathbf{X}_W^{2\bullet}$ considered in Section 2.3, the choice of orientation is determined by an independent fair coin flip. On rigorous grounds, the mapping ϕ allows this choice to be done in a measurable way.

As an immediate consequence, we have the following. Recall that $\mathbb{P}_{\text{Sphere}}^{2\bullet}$ is the image measure $\psi_*\mathbb{P}_{\text{Snake}}$.

Corollary 6. *The measure $\mathbb{P}_{\text{Snake}}$ is the image measure of $\mathbb{P}_{\text{Sphere}}^{2\bullet} \otimes (\delta_{-1} + \delta_1)/2$ under the mapping ϕ .*

Remark. We mention that the choice of the random variable ϵ_h is not canonical. Theorem 4 would remain true (although for a possibly different inverse function ϕ) if we had adopted some other definition than (3), as long as it almost surely differentiates h from $R(h)$. However, for a choice of ϵ_h not satisfying the additional property (5), Corollary 6 would not be true.

3.2 The role of the marked points

The role of ϵ being now (partially) clarified, let us address the role of the distinguished points x_W^0, x_W^1 . Recall the notation $\mathbb{P}_{\text{Sphere}}$ for the law of the *unmarked* Brownian sphere.

By the re-rooting property [13], conditionally given $[X, d, \mu]$ with law $\mathbb{P}_{\text{Sphere}}$, if y^0 and y^1 are two independent random points in X with law μ , then $[X, d, \mu, y^0, y^1]$ has law $\mathbb{P}_{\text{Sphere}}^{2\bullet}$. In other words, the points x_W^0, x_W^1 play the role of two independent marked points, distributed according to the area measure³.

Summarizing the discussion of this and the preceding sections, we arrive at the following statement, which is a more precise version of Theorem 1.

Corollary 7. *Let $\mathbf{X} = [X, d, \mu]$ have law $\mathbb{P}_{\text{Sphere}}$. Conditionally given \mathbf{X} , let x^0, x^1 be two independent random points in X with law μ . Let $W_{\pm} = \phi(\mathbf{X}^{2\bullet}, \pm 1)$, where $\mathbf{X}^{2\bullet} = [X, d, \mu, x^0, x^1]$. Then, almost surely, $R(W_+) = W_-$ and $\psi(W_+) = \psi(W_-) = \mathbf{X}^{2\bullet}$. Moreover, if $\sigma \in \{+, -\}$ is itself random, independent of $\mathbf{X}^{2\bullet}$, and uniformly distributed, then W_{σ} has law $\mathbb{P}_{\text{Snake}}$.*

3.3 The role of the measure

Finally, let us discuss the role of the area measure μ . As shown by Le Gall [15], this measure is almost surely determined by the metric structure, in the following sense. Fix the gauge function $H(r) = r^4 \log \log(1/r)$. Then there exists a constant $c \in (0, \infty)$ such that $\mathbb{P}_{\text{Snake}}(dh)$ -a.s., μ_h is equal to c times the H -Hausdorff measure on the space (X_h, d_h) . Hence the mapping $[X, d, \mu] \mapsto [X, d]$ from the Gromov–Hausdorff–Prokhorov space $m\mathcal{M}$ to the Gromov–Hausdorff space \mathcal{M} is injective on a Borel set of full measure.

Therefore, by the Lusin–Souslin theorem (already mentioned in Section 3 above), there exists a Borel mapping $\chi : \mathcal{M} \rightarrow m\mathcal{M}$ such that $\chi([X, d]) = [X, d, \mu]$, and $\mathbb{P}_{\text{Sphere}}^{\circ}(d[X, d])$ -a.s., where $\mathbb{P}_{\text{Sphere}}^{\circ}$ is the law of the unmeasured space $[X_h, d_h]$ under $\mathbb{P}_{\text{Snake}}(dh)$. Given these observations, it is possible to state a version of Corollary 7, with $\mathbb{P}_{\text{Sphere}}$ replaced by $\mathbb{P}_{\text{Sphere}}^{\circ}$. We omit the details.

³Strictly speaking, this discussion is not completely accurate since we are working with isometry classes of spaces, and not with fixed space. A more precise statement would be in terms of Markov kernels $m\mathcal{M} \rightarrow m\mathcal{M}^{2\bullet}$; see [18, Section 6.5]. However, for ease of exposition, we will use to this slightly informal formulation.

4 Proof of Theorem 4

Recall that, by virtue of the Lusin–Souslin theorem, it suffices to prove that, for $\mathbb{P}_{\text{Snake}}$ -a.e. $h = (f, g) \in \mathcal{S}$, the functions f and g can be expressed as a function of $\mathbf{X}_h^{2\bullet}$ and ϵ_h .

From now on, we let $W = (\mathbf{e}, Z)$ be a random variable with law $\mathbb{P}_{\text{Snake}}$ defined on some probability space, and our goal is to show that W is determined by $\mathbf{X}_W^{2\bullet}, \epsilon_W$ on a set of full probability. We prove this by following the steps listed in Section 1.1.

4.1 The two intertwined trees

If (\mathcal{T}, d) is an \mathbb{R} -tree and $x \in \mathcal{T}$, we let $\deg_{\mathcal{T}}(x) \in \{1, 2, \dots\} \cup \{\infty\}$ be the number of connected components of $\mathcal{T} \setminus \{x\}$. The sets

$$\text{Leaf}(\mathcal{T}) = \{x \in \mathcal{T} : \deg_{\mathcal{T}}(x) = 1\} \quad \text{and} \quad \text{Skel}(\mathcal{T}) = \mathcal{T} \setminus \text{Leaf}(\mathcal{T})$$

are called the set of *leaves* and the *skeleton* of \mathcal{T} . We will use the well-known fact that if $f : [0, 1] \rightarrow \mathbb{R}$ is a continuous function with $f(0) = f(1) = 0$, then the points of $\text{Skel}(\mathcal{T}_f)$ are exactly those which have at least two preimages in $[0, 1)$ under p_f .

Our proof of Theorem 4 will depend a great deal on the fact that the images of the trees $\text{Skel}(\mathcal{T}_{\mathbf{e}})$ and $\text{Skel}(\mathcal{T}_Z)$ under the projections $\mathbf{p}_{\mathbf{e}}$ and \mathbf{p}_Z are geometric loci in the Brownian sphere. Namely, almost surely, the first one is the cut locus of (X_W, d_W) with respect to the point x_W^1 , and the second is the set of relative interiors of geodesics towards x_W^1 . These properties are already known, and summarized as follows.

Lemma 8. *The following properties hold almost surely.*

- (i) *The restrictions of $\mathbf{p}_{\mathbf{e}}$ and \mathbf{p}_Z to $\text{Skel}(\mathcal{T}_{\mathbf{e}})$ and $\text{Skel}(\mathcal{T}_Z)$ are homeomorphisms onto their images, which we denote by C_W and Γ_W , respectively.*
- (ii) *The set C_W is the cut locus of (X_W, d_W) with respect to x_W^1 , which consists of the points $x \in X_W$ such that there exists at least two distinct geodesic paths from x to x_W^1 .*
- (iii) *The set Γ_W (of points “inside” geodesics to x_W^1) consists of the points $x \in X_W$ such that there exists a geodesic segment in (X_W, d_W) that contains x , and whose extremities are x_W^1 and some other point $y \neq x$.*
- (iv) *It holds that $C_W \cap \Gamma_W = \emptyset$, and moreover, for every $x \in X_W \setminus \Gamma_W$ (resp. $x \in X_W \setminus C_W$), x has a unique preimage under $\mathbf{p}_{\mathbf{e}}$ (resp. \mathbf{p}_Z).*

For convenience, let us also define

$$\tilde{X}_W = X_W \setminus (C_W \cup \Gamma_W).$$

See Figure 1 for an illustration of the above results.

Proof. Points (i)–(iii) are proved in [13, Proposition 3.1] and [20, Theorem 6.3.3]. More precisely, it holds that the geodesic segments to x_W^1 in (X_W, d_W) are exactly of the form $\mathbf{p}_Z([\rho_Z, a]_Z)$, where $a \in \mathcal{T}_Z$, which are called the *simple geodesics* in [13], and one has $d_W(x_W^1, \mathbf{p}_Z(a)) = d_Z(\rho_Z, a)$.

Point (iv) is a consequence of [12, Theorem 3.4] and [16, Lemma 3.2]. Let us give a bit more details on this last point. The two aforementioned results can be reformulated as follows: for every $s \neq t$ in $(0, 1)$, one has $d_W(s, t) = 0$ if and only if $d_e(s, t) = 0$ or $d_Z(s, t) = 0$, these two possibilities being mutually exclusive, and, given the characterization of $\text{Skel}(\mathcal{T}_f)$ recalled at the beginning of this subsection, this implies directly that $C_W \cap \Gamma_W = \emptyset$. Moreover, if $a \neq b$ are elements of \mathcal{T}_e such that $\mathbf{p}_e(a) = \mathbf{p}_e(b) = x$, then we can find $s \neq t \in [0, 1)$ such that $p_e(s) = a$, $p_e(t) = b$. Then it holds that $d_W(s, t) = 0$, but $d_e(s, t) > 0$, which implies that $d_Z(s, t) = 0$, meaning that $x \in \Gamma_W$. The argument is completely symmetric and can be applied to give the last property. \blacksquare

4.2 Recovering the tree branches

Working on the almost sure event that the properties of Lemma 8 hold, one can define distinguished simple paths in the Brownian sphere. For $x, y \in X_W \setminus \Gamma_W$, we let

$$C_W(x, y) = \mathbf{p}_e([\mathbf{p}_e^{-1}(x), \mathbf{p}_e^{-1}(y)]_e).$$

Likewise, for $x, y \in X_W \setminus C_W$, we define

$$\Gamma_W(x, y) = \mathbf{p}_Z([\mathbf{p}_Z^{-1}(x), \mathbf{p}_Z^{-1}(y)]_Z).$$

Note that $C_W(x, y)$ and $\Gamma_W(x, y)$ are simple curves in X_W , by Lemma 8(i).

Lemma 9. *Almost surely, it holds that:*

- (i) *For every $x, y \in X_W \setminus C_W$, the two geodesics from x and y to x_W^1 , meet for the first time at some point $z \in \Gamma_W$. The set $\Gamma_W(x, y)$ is the union of the geodesic segment from x to z and the geodesic segment from y to z , and*

$$d_Z(\mathbf{p}_Z^{-1}(x), \mathbf{p}_Z^{-1}(y)) = d_W(x, z) + d_W(y, z). \quad (8)$$

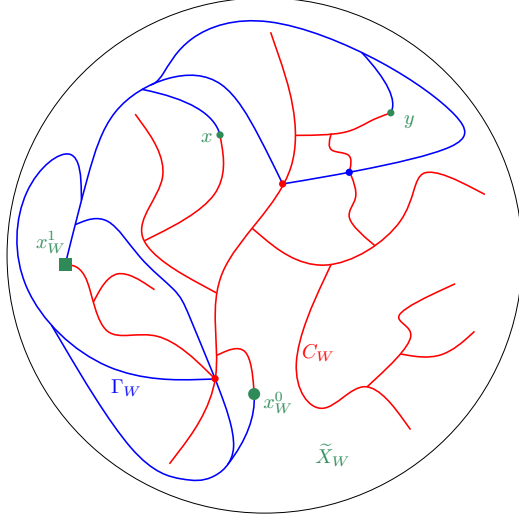


Figure 1: Some branches of the tree Γ_W of relative interiors of geodesics toward x_W^1 are represented in blue, and a part of the the cut locus C_W is represented in red. The two distinguished points x_W^0 and x_W^1 are almost surely not in $\Gamma_W \cup C_W$, and we have represented two more points x, y outside this set.

(ii) For every $x, y \in X_W \setminus \Gamma_W$, the set

$$C_W(x, y) \setminus \{x, y\} \subset C_W$$

is the set of points z such that there exist two geodesics from z to x_W^1 that separate x and y (meaning that the points x and y lie in different connected components of the complement of the geodesics).

This lemma is illustrated in Figure 2.

Proof. The first point (i) is proved in [19, Lemmas 4 and 5], but we recall the main ideas. We use the fact that $\Gamma_W(x, x_W^1)$ is a geodesic path in (X_W, d_W) , isometric to the segment $[[\mathbf{p}_Z^{-1}(x), \rho_Z]]_Z$ in (\mathcal{T}_Z, d_Z) . The fact that \mathcal{T}_Z is an \mathbb{R} -tree shows that the paths $\Gamma_W(x, x_W^1)$ and $\Gamma_W(y, x_W^1)$ coincide on a maximal final segment of the form $\Gamma_W(z, x_W^1)$. Moreover, one has

$$\begin{aligned} d_Z(\mathbf{p}_Z^{-1}(x), \mathbf{p}_Z^{-1}(y)) &= d_Z(\mathbf{p}_Z^{-1}(x), \mathbf{p}_Z^{-1}(z)) + d_Z(\mathbf{p}_Z^{-1}(y), \mathbf{p}_Z^{-1}(z)) \\ &= d_W(x, z) + d_W(y, z). \end{aligned}$$

For the second point (ii), we first observe that if $z \notin C_W(x, y) \setminus \{x, y\}$, then the continuous path $C_W(x, y)$ connects x and y without intersecting

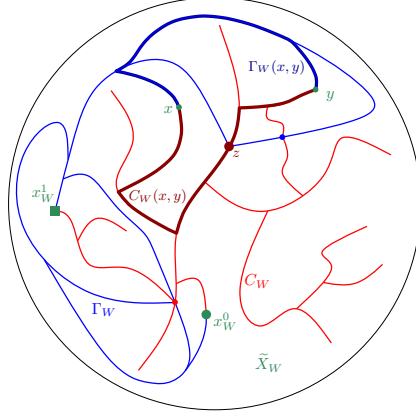


Figure 2: From the points $x, y \in \tilde{X}_W$, there is a unique geodesic pointing towards x_W^1 , which allows to identify $\Gamma_W(x, y)$, represented by the thick dark blue line. The curve $C_W(x, y)$, represented by the thick dark red line, consists of points from which we can find (at least) two geodesics pointing towards x_W^1 that separate x from y . One of these points, called z , is highlighted together with the two relevant geodesics.

z (except possibly at its extremities) nor Γ_W because of Lemma 8(iv). In particular, the geodesics from z do not disconnect x from y .

Conversely, let $z \in C_W(x, y) \setminus \{x, y\}$, and let $a = \mathbf{p}_e^{-1}(x)$ and $b = \mathbf{p}_e^{-1}(y)$. Note that $c = \mathbf{p}_e^{-1}(z)$, being an element of $\text{Skel}(\mathcal{T}_e)$, splits the latter into two or three connected components. Let us assume for simplicity that we are in the first case (the case of three components can be treated similarly). This means that there exist exactly two times $u \neq u' \in (0, 1)$ such that $p_e(u) = p_e(u') = c$. Our goal is to show that the union of the two geodesic segments $\mathbf{p}_Z([p_Z(u), \rho_Z])_Z$ and $\mathbf{p}_Z([p_Z(u'), \rho_Z])_Z$ from z to x_W^1 in (X_W, d_W) separates x from y . Note that these two paths form a “lollipop” shape: they both start from z , remain disjoint in a neighborhood of z , and then merge into a final common segment, and consequently, they indeed separate X_W into two connected components.

In order to show that x and y do not belong to the same connected component, we consider a continuous path $\alpha : [0, 1] \rightarrow X_W$ from x to y , and aim to show that α intersects the union of geodesics from z to x_W^1 in (X_W, d_W) . Let us call $\mathcal{T}_e(a)$ (resp. $\mathcal{T}_e(b)$) the component of $\mathcal{T}_e \setminus \{c\}$ containing a (resp. b). Let $r_0 = \inf\{r \in [0, 1] : \mathbf{p}_e^{-1}(\alpha(r)) \in \mathcal{T}_e(b)\}$. Then there exist sequences $(r_n), (r'_n)$ that are respectively non-decreasing and non-increasing with limit r_0

such that $\mathbf{p}_e^{-1}(\alpha(r_n)) \in \mathcal{T}_e(a)$ and $\mathbf{p}_e^{-1}(\alpha(r'_n)) \in \mathcal{T}_e(b)$ for every n , and up to extracting a subsequence, we may assume that the latter sequences converge to $a' \in \mathcal{T}_e(a) \cup \{c\}$ and $b' \in \mathcal{T}_e(b) \cup \{c\}$, such that $\mathbf{p}_e(a') = \mathbf{p}_e(b') = \alpha(r_0)$.

If $\alpha(r_0) = z$, then we obtain the desired conclusion. Otherwise, we have $a' \in \mathcal{T}_e(a)$ and $b' \in \mathcal{T}_e(b)$, and this implies the existence of $s', t' \in [0, 1]$ such that $p_e(s') = a'$ and $p_e(t') = b'$, and $d_W(s', t') = 0$ (since a' and b' both project to $\alpha(r_0)$ via \mathbf{p}_e). We know that this implies that $d_e(s', t') = 0$ or $d_Z(s', t') = 0$, but the first case is excluded since $a' \neq b'$. This means that $Z_{s'} = Z_{t'} = \min_{[s', t']_\circ} Z$ or $Z_{s'} = Z_{t'} = \min_{[t', s']_\circ} Z$, depending on which of the minima is the largest one (recalling the notation for cyclic intervals from Section 2.1.1). Since c is on the path of \mathcal{T}_e from a to b , it must hold that one of u or u' is in $[s', t']_\circ$, and the other one is in $[t', s']_\circ$. This implies that $p_W(s') = p_W(t')$ is on the simple geodesic from u or from u' , as desired. ■

4.3 Orienting the sphere and recovering Z

In this section, we explain how one can recover the process Z from $(\mathbf{X}_W^{2\bullet}, \epsilon_W)$. Recall that, a.s., $x_W^0, x_W^1 \in \tilde{X}_W$. The preceding lemma allows to describe C_W , Γ_W , \tilde{X}_W , and the segments $C_W(x, y)$ and $\Gamma_W(x, y)$ for $x, y \in \tilde{X}_W$, in terms of $(X_W, d_W, \mu_W, x_W^0, x_W^1)$, in a way that is invariant with respect to isometries. That is, if we select an element (X, d, μ, x^0, x^1) in the isometry class $\mathbf{X}_W^{2\bullet}$, then we can define sets C, Γ, \tilde{X} , and $C(x, y)$ and $\Gamma(x, y)$ for every $x, y \in \tilde{X}$, in such a way that a measure-preserving isometry from $(X_W, d_W, \mu_W, x_W^0, x_W^1)$ to (X, d, μ, x^0, x^1) sends C_W to C , Γ_W to Γ , etc. This will be crucial in our main proof.

Lemma 10. *Almost surely, for every $x \in \tilde{X}_W \setminus \{x_W^0\}$, the curve $\gamma(x) = C_W(x_W^0, x) \cup \Gamma_W(x, x_W^0)$ is a closed, simple loop in X_W , and $p_W([0, p_W^{-1}(x)])$ and $p_W([p_W^{-1}(x), 1])$ are the closures of the two Jordan domains that it separates.*

Proof. Let $x \in \tilde{X}_W$ and $s = p_W^{-1}(x)$. Observe that the two closed simple curves $C_W(x_W^0, x)$ and $\Gamma_W(x, x_W^0)$ intersect only at their extremities, since $C_W \cap \Gamma_W = \emptyset$ and $x_W^0 \in \tilde{X}_W$. As a consequence, their union $\gamma(x)$ forms a simple loop separating two disks in X_W . Furthermore, the sets $p_W([0, s])$ and $p_W([s, 1])$ are compact and connected, with union X_W . Therefore, it suffices to show that their boundary is $\gamma(x)$.

To this end, we proceed similarly to the proof of Lemma 9. We let $\alpha : [0, 1] \rightarrow X_W$ be a continuous path with $\alpha(0) \in p_W([0, s]) \setminus \gamma(x)$ and

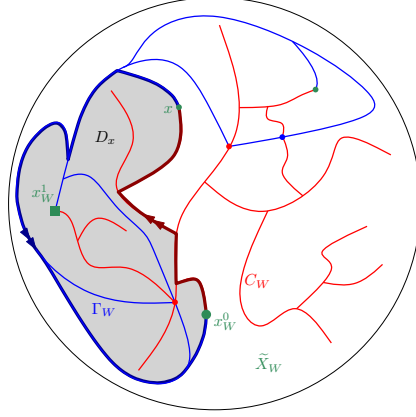


Figure 3: The curve $\gamma(x)$ is illustrated in thick lines, and the domain $D_x = p_W([0, p_W^{-1}(x)])$ is the gray area. If we choose to orient the curve $\gamma(x)$ by first following $C_W(x_W^0, x)$ from x_W^0 to x , then the Brownian sphere is canonically oriented in such a way that D_x is circled counterclockwise by $\gamma(x)$, for any choice of $x \in \tilde{X}_W \setminus \{x_W^0\}$.

$\alpha(1) \in p_W([s, 1]) \setminus \gamma(x)$, and we aim to prove that α intersects $\gamma(x)$. Let $r_0 = \inf\{r \in [0, 1] : \alpha(r) \in p_W([s, 1])\}$. Then, by compactness, there must exist $s' \in [0, s]$ and $t' \in [s, 1]$ such that $p_W(s') = p_W(t') = \alpha(r_0)$. If s' or t' equals s , then this means that $\alpha(r_0) = x$ and we are done. Otherwise, we know that either $d_e(s', t') = 0$ or $d_Z(s', t') = 0$. In the first case, we deduce $\alpha(r_0) \in C_W(x_W^0, x)$, and in the second case, $\alpha(r_0) \in \Gamma_W(x, x_W^0)$, which concludes the proof. \blacksquare

For a given $x \in \tilde{X}_W \setminus \{x_W^0\}$, we may choose the orientation of X_W such that the loop $\gamma(x)$, oriented by following the segment $C_W(x_W^0, x)$ from x_W^0 to x and $\Gamma_W(x, x_W^0)$ from x to x_W^0 , goes around $p_W([0, p_W^{-1}(x)])$ counterclockwise.

We claim that this choice of orientation is independent of x . To see this, note that if $p_W^{-1}(x) < p_W^{-1}(x')$, we have that

$$p_W([0, p_W^{-1}(x)]) \subset p_W([0, p_W^{-1}(x')]),$$

and that the paths $C_W(x_W^0, x)$ and $C_W(x_W^0, x')$ have nontrivial intersection, and similarly for $\Gamma_W(x, x_W^0)$ and $\Gamma_W(x', x_W^0)$. The argument is similar if $p_W^{-1}(x') < p_W^{-1}(x)$. See Figure 3 for an illustration of the above discussion.

This being said, we cannot a priori distinguish the two regions only from the isometry class $\mathbf{X}_W^{2\bullet}$. This is where the sign variable ϵ_W defined at (3) comes

into play. In order to make this specific choice of orientation, we take $x = x_W^1$ as a reference point, and decide that, among the two regions separated by $\gamma(x_W^1)$, the region circled counterclockwise by $\gamma(x_W^1)$ is the one of smallest μ_W -measure if $\epsilon_W = 1$, or the one of largest μ_W -measure if $\epsilon_W = -1$. There is an ambiguity when both regions have the same measure, but this happens with probability 0 since $s_* = s_*(W)$ is a uniform random variable in $[0, 1]$. In this way, we see that it is indeed possible to identify the region $p_W([0, s_*])$, and hence, the canonical orientation of X_W .

Once this orientation choice is made, we can finally recover the process Z as follows. For each $x \in \tilde{X}_W$, we define D_x to be the disk in X_W bounded by $C_W(x_W^0, x) \cup \Gamma_W(x, x_W^0)$, and such that the loop $\gamma(x)$ goes around D_x in counterclockwise order, for the canonical orientation. From the above discussion, it holds that $D_x = p_W([0, p_W^{-1}(x)])$, and therefore, we see that we can identify $p_W^{-1}(x)$ purely in metric-measure terms, as follows.

Corollary 11. *Almost surely, it holds that*

$$\forall x \in \tilde{X}_W, \quad p_W^{-1}(x) = \mu_W(D_x).$$

We have thereby identified $p_W^{-1}(\tilde{X}_W)$, the restriction of p_W to $p_W^{-1}(\tilde{X}_W)$, and the restriction of Z to $p_W^{-1}(\tilde{X}_W)$, using (8) and the observation that

$$Z_s - Z_{s_*(W)} = d_Z(\mathbf{p}_Z^{-1}(p_W(s)), \mathbf{p}_Z^{-1}(x_W^1)), \quad s \in p_W^{-1}(\tilde{X}_W).$$

The functions p_W and Z can then be extended by continuity to $[0, 1]$.

We conclude this section by noting, as stressed in the previous section, that our constructions are invariant with respect to isometries. That is, applying them to any choice of element in the isometry class $\mathbf{X}_W^{2\bullet}$ produces the same function Z .

4.4 Recovering \mathbf{e}

It remains to determine \mathbf{e} on $[0, 1]$, which requires a slightly different argument since there is no formula similar to (8) for expressing the distance $d_{\mathbf{e}}$ directly in terms of $[X_W, d_W]$. As noted, the idea here is that \mathbf{e} encodes a known continuum tree, and we are also provided with the values of the Brownian snake parametrized by that tree. Thus in order to recover \mathbf{e} we just need to know the length of paths in the tree. These can be deduced from the

Brownian snake by measuring its quadratic variation. See Lemma 12 for this last step. We proceed to make this precise.

First, we note that it suffices to determine \mathbf{e} on $\mathbb{Q} \cap [0, 1]$, as \mathbf{e} can then be extended to $[0, 1]$ by continuity. Observe that $p_W(\mathbb{Q} \cap [0, 1]) \subset \tilde{X}_W$, almost surely⁴. Consider the function ℓ on X_W defined by

$$\ell(x) = d_W(x, x_W^1) - d_W(x_W^0, x_W^1).$$

Fix $q \in \mathbb{Q} \cap [0, 1]$, and let $\beta_q(r) = \sup\{t \leq q : \mathbf{e}_t = r\}$ for $0 \leq r \leq \mathbf{e}_q$. Then $p_{\mathbf{e}} \circ \beta_q$ is isometric with image $[[\rho_{\mathbf{e}}, p_{\mathbf{e}}(q)]]_{\mathbf{e}}$ in $(\mathcal{T}_{\mathbf{e}}, d_{\mathbf{e}})$, so that $p_W \circ \beta_q$ is a natural parametrization of $C_W(x_W^0, p_W(q))$ by $[0, \mathbf{e}_q]$. By the defining properties of (\mathbf{e}, Z) and formula (8), the mapping $B^{(q)} = \ell \circ p_W \circ \beta_q$ is a standard Brownian motion with duration \mathbf{e}_q , conditionally on \mathbf{e} .

Since we do not know \mathbf{e} a priori from $(\mathbf{X}_W^{2\bullet}, \epsilon_W)$, we do not have direct access to β_q . However, if α_q is any parametrization of $C_W(x_W^0, p_W(q))$ (by $[0, 1]$, say), then $\ell \circ \alpha_q$ is a time-change of this Brownian motion. This means that $(\mathbf{X}_W^{2\bullet}, \epsilon_W)$ determines $B^{(q)}$ up to reparametrization, for every $q \in \mathbb{Q} \cap [0, 1]$.

Lemma 12. *Let $B = (B_t, t \geq 0)$ be a standard Brownian motion. Then, almost surely, the following property holds. For every increasing continuous function $\kappa : [0, 1] \rightarrow \mathbb{R}_+$ with $\kappa(0) = 0$, it is possible to compute $\kappa(1)$ as a function of $(B_{\kappa(u)}, 0 \leq u \leq 1)$.*

Proof. Consider the number of steps made by $(B_{\kappa(u)}, 0 \leq u \leq 1)$ on the sub-lattice $\varepsilon\mathbb{Z}$, multiply by ε^2 , and then take a limit. \blacksquare

From this observation, we deduce that almost surely, $(\mathbf{e}_q, q \in \mathbb{Q} \cap [0, 1])$ can be recovered from the isometry class $\mathbf{X}_W^{2\bullet}$ and ϵ_W . Finally, we conclude that $W = (\mathbf{e}, Z)$ is a function of ϵ_W and the isometry class $\mathbf{X}_W^{2\bullet}$, rather than of some particular representative. This completes the proof.

⁴There is a small subtlety here: the information given by the dense set $p_W(\mathbb{Q} \cap [0, 1])$ is not obviously invariant under isometries. The reason why this indeed holds is that we have identified the parametrization by $[0, 1]$ (i.e., the measure and order structure) in the previous subsection, so we can define “the point visited at time $q \in \mathbb{Q}$ ” by p_W in purely measure-metric terms.

References

1. D. Aldous. The continuum random tree. I. *Ann. Probab.*, 19(1):1–28, 1991.
2. D. Aldous. The continuum random tree. II. An overview. In *Stochastic analysis (Durham, 1990)*, volume 167 of *London Math. Soc. Lecture Note Ser.*, pages 23–70. Cambridge Univ. Press, Cambridge, 1991.
3. D. Aldous. The continuum random tree. III. *Ann. Probab.*, 21(1):248–289, 1993.
4. E. Baur, G. Miermont, and G. Ray. Classification of scaling limits of uniform quadrangulations with a boundary. *Ann. Probab.*, 47(6):3397–3477, 2019.
5. J. Bettinelli and G. Miermont. Compact Brownian surfaces II. Orientable surfaces. Available at arXiv:2212.12511.
6. J. Bettinelli and G. Miermont. Compact Brownian surfaces I: Brownian disks. *Probab. Theory Related Fields*, 167(3-4):555–614, 2017.
7. L. Chaumont and G. Uribe Bravo. Shifting processes with cyclically exchangeable increments at random. In *XI Symposium on Probability and Stochastic Processes*, volume 69 of *Progr. Probab.*, pages 101–117. Birkhäuser/Springer, Cham, 2015.
8. R. Cori and B. Vauquelin. Planar maps are well labeled trees. *Canadian J. Math.*, 33(5):1023–1042, 1981.
9. N. Curien and J.-F. Le Gall. The Brownian plane. *J. Theoret. Probab.*, 27(4):1249–1291, 2014.
10. A. S. Kechris. *Classical descriptive set theory*, volume 156 of *Graduate Texts in Mathematics*. Springer-Verlag, New York, 1995.
11. J.-F. Le Gall. A class of path-valued Markov processes and its applications to superprocesses. *Probab. Theory Related Fields*, 95(1):25–46, 1993.
12. J.-F. Le Gall. The topological structure of scaling limits of large planar maps. *Invent. Math.*, 169(3):621–670, 2007.

13. J.-F. Le Gall. Geodesics in large planar maps and in the Brownian map. *Acta Math.*, 205(2):287–360, 2010.
14. J.-F. Le Gall. Uniqueness and universality of the Brownian map. *Ann. Probab.*, 41(4):2880–2960, 2013.
15. J.-F. Le Gall. The volume measure of the Brownian sphere is a Hausdorff measure. *Electron. J. Probab.*, 27:Paper No. 113, 28, 2022.
16. J.-F. Le Gall and F. Paulin. Scaling limits of bipartite planar maps are homeomorphic to the 2-sphere. *Geom. Funct. Anal.*, 18(3):893–918, 2008.
17. J.-F. Le Gall and M. Weill. Conditioned Brownian trees. *Ann. Inst. H. Poincaré Probab. Statist.*, 42(4):455–489, 2006.
18. G. Miermont. Tessellations of random maps of arbitrary genus. *Ann. Sci. Éc. Norm. Supér. (4)*, 42(5):725–781, 2009.
19. G. Miermont. The Brownian map is the scaling limit of uniform random plane quadrangulations. *Acta Math.*, 210(2):319–401, 2013.
20. G. Miermont. Aspects of random maps. Lecture notes of the Saint-Flour Summer School 2014, available at <http://perso.ens-lyon.fr/gregory.miermont/coursSaint-Flour.pdf>, 2014.
21. J. Miller and S. Sheffield. Liouville quantum gravity and the Brownian map I: the QLE(8/3, 0) metric. *Invent. Math.*, 219(1):75–152, 2020.
22. J. Miller and S. Sheffield. Liouville quantum gravity and the Brownian map II: Geodesics and continuity of the embedding. *Ann. Probab.*, 49(6):2732–2829, 2021.
23. J. Miller and S. Sheffield. Liouville quantum gravity and the Brownian map III: the conformal structure is determined. *Probab. Theory Related Fields*, 179(3-4):1183–1211, 2021.
24. G. Schaeffer. *Conjugaison d’arbres et cartes combinatoires aléatoires*. PhD thesis, Université Bordeaux I, 1998.